Frontiers in Scientific Research and Technology

Online ISSN: 2682-2970
Print ISSN: 2682-2962
http://fsrt.journals.ekb.eg

FSRT J 9 (2024) 117 - 127 10.21608/fsrt.2024.311622.1134

Optical bistabilities in cavity optomechanics

Y. A. Sharaby[1], I. M. Kandil[1,*], A. A. Mohamed[1] ,and S. S. Hassan[2]

[1] Physics Department, Faculty of Science, Suez University, P.O. Box 43221 Suez, Egypt.

[2] Independent Researcher, 237 Banafseg 7, New Cairo, Egypt.

ARTICLE INFO

Article history:
Received 11 August 2024
Received in revised form 17 August 2024
Accepted 24 August 2024
Available online 26 August 2024

Keywords
Optical bistability,
Optomechanical system,
Inhomogeneous broadening.

ABSTRACT

In this review, we focused our study on the optical bistability of an optomechanical cavity and derived a mathematical equation that predicts the system behavior. We began with the study of optical bistability for conventional optomechanical systems, then we studied a hybrid optomechanical cavity, by embedding with N 2-level atoms to the conventional optomechanical cavity. Finally, we studied n optomechanical system embedded with N 2-level inhomogeneous broadened atoms. For each system, we start with calculating the Heisenberg-Langevin equations that describe the dynamics of the system, then solving the equation in the steady state condition using Fourier series decomposition up to the first harmonics [1,2]. Lastly, we derived an equation that predicts the behavior of the system either bistable, transistor, or monostable for each system from the value of the system parameters. Investigating the relations between all the physical dynamical variables in the optomechanical system against the incident field intensity, we conclude that all the system variable relation with the incident field intensity is dependent on the fundamental optical cavity output field component against the incident field intensity. Finally, we studied the effects of integrating an atomic media into the optomechanical system and the tunability it could provide to the optomechanical system. The atomic medium tends to squeeze the domain of the bistability within the system relative to the conventional optomechanical system.

1. Introduction

1.1 Brief introduction to optomechanical system

Optomechanics studies the systems where a non-linear coupling between the optical field and mechanical vibration modes occurs as a result of the radiation pressure[3]. The conventional optomechanical system is composed of a Fabry-Perot cavity with one of the parallel mirrors that is allowed to oscillate freely, as it is connected to the wall by a spring. The radiation pressure exerted by the cavity field on the freely oscillating mirror creates or attenuates the mechanical mode of vibration, this shapes the non-linear coupling between the optical field within the cavity and the mechanical mode and leads to numerous fascinating quantum phenomena, such as the detection of gravity waves[4, 5], cooling via radiation pressure [6,7], sensing small mechanical displacements and forces [3]. Many optomechanical behaviors were opened for the researchers to study, e.g. bistability and multistability [8-10], optomechanical induced transparency (OMIT) [5,11-14], optical amplification [13-15], and slow light [16].

A hybrid optomechanical system is a conventional optomechanical system combined with an atomic medium. This atomic medium could vary from a single 2-level atom embedded in the cavity or coupled to the movable mirror [9,11-14,15-18], a photonic crystal [19], a quantum dot (QD) [10,20-25], or an ensemble of atoms [4,7,9,14,16,17]. Another form of a hybrid optical cavity is composed of two or more conventional optical cavities coupled [9,20,24,26]. Hybrid optomechanical cavities are used to either introduce new behavior, tune the system's current behavior, or a combination of both.

1.2 Literature review

The Fabry-Perot optical cavity is an old concept that many physicists used since 1899, on the other hand, Kepler introduced the radiation pressure concept in the 17th century as an interpretation of the observation of the dust tails of comets that point away from the sun during a comet transit [27], he postulated that light has a momentum which gives rise to the ability of radiation to apply forces. In 1909, Einstein derived statistics of the radiation pressure force fluctuations acting on a moveable mirror [28], including the frictional effects of the radiation force, due to this analysis Einstein was allowed to reveal the dual wave-particle nature of blackbody radiation. Despite the old concepts the combination of the radiation pressure within

* Corresponding author at Suez University

E-mail addresses: ibrahim.kandil@suezuni.edu.eg (Ibrahim M. Kandil)

the optical cavity was introduced experimentally in 1983, where the optical bistability as a result of radiation pressure was first demonstrated in the first optomechanical cavity experiment[29].

The fundamental effects of quantum fluctuations in radiation pressure were labeled by Braginsky, revealing the imposed limits on the accuracy of measuring the position of a free test mass (such as a mirror) [30,31]. An analysis held by Caves shows in detail the role of this ponderomotive quantum noise in interferometers [32]. This work found the standard quantum limit for continuous position measurements, essential for gravitational wave detectors such as LIGO and VIRGO.

In the 1990s, many optomechanical quantum cavity systems start to be explored theoretically. An example of these is light squeezing [33,34] and quantum mechanical nondestructive detection (QND) of light intensity [35,36].

Experimentally, the cooling based on radiation pressure was demonstrated for the first time in [37] for the vibrational modes of a macroscopic end mirror. This reaches lower temperatures later in the studies [38,39]. At the same time, there was a trend towards miniaturization of mechanical elements: for example, the thermal behavior of a mm mirror was monitored in a cryogenic optical cavity [40]. However, fabricating high-quality optical Fabry-Pérot resonators below this scale proved to be a major challenge. Nevertheless, it has been possible to observe the photomechanical effects of delayed radiation forces in microassemblies where the force is of photothermal origin, effectively replacing the cavity lifetime with a thermal time constant. Examples include the optical spring effect [1], feedback damping [41], spontaneous oscillations [42,43], and the demonstration of cavity cooling by dynamic feedback of delayed photothermal optical forces [44,45].

In 2005, the optical microtoroid resonators were discovered to have high optical finesse, while containing mechanical modes and hence can exhibit optomechanical effects, in particular the self-oscillation induced radiation pressure[1,46,47] (i.e., what Braginsky designated "parametric instability"). Since then, several systems have reported the rapid development of the optomechanical cavity and optomechanical coupling. These include membranes of Fabry-Perot resonators [48] and nanorods [49], photonic crystals [50], whispering gallery microdisks [51,52] and microspheres [53-55], and evanescently coupled nanobeams [56]. Furthermore, cavity optomechanics has been demonstrated for the mechanical excitation of cold atomic clouds [57,58].

Optical bistability is a phenomenon where the optical cavity undergoes a transition from a lower state to a higher state or vice versa, forming discontinuous changes or a hysteresis relation between the input-output field's relation. This phenomenon was predicted in 1969 by SZokE and his colleagues[59-62]. A few years later, McCall [63] studied optical bistability numerically in a Fabry-Perot cavity, suggesting the GIBBS, MoCA LL, and VENKA TESAN experiments in Na and Ruby, where the first bistable responses were observed at well times [64,65]. These experiments showed that this system is the basis for a whole range of device applications, such as optical memories, optical transistors, clippers, and limiters. These important results stimulated a very active theoretical study that diverged in two directions. The first direction was mainly interested in the device aspects of this phenomenon, in particular investigating the feasibility of electro-optical systems for generating bistability and related phenomena. An overview of this approach can be found in [66]. The second direction [67-69] examines optical bistability as a fundamental chapter in the interaction between polyatomic systems and radiation. More precisely, he considers optical bistable systems as a passive counterpart of lasers. Optical bistability is contributing to many recent applications in quantum computing systems such as memory [70,71], optical communication [72], and optical switching[70].

1.3 Organization of the review

In this review we introduced the optical bistability OB for a simple optical cavity system model for all the fundamental and first harmonic component parameters, presenting the dependency of all the components on the fundamental cavity field component. Then a mathematical condition for optical bistability has been deduced and the different behavior condition values in sub-section 2.1. In section 2.2 we study a hybrid optomechanical system embedded with N 2-level atoms, studying the optical bistability for input-output relation (i.e. fundamental component of cavity field against the incident controlled field), reduce the mathematical condition for optical bistability and discuss the effect of the atomic medium cavity field coupling constant. In section 2.3 we introduced atomic medium broadening and its effect on the optical bistability. In conclusion, we summarized the effect of adding an atomic medium on tuning the optical bistability.

2. Formulation and results

2.1 Optical bistability for basic optical cavity system

At first, a simple optomechanical model is considered, consisting of a Fabry-Perot cavity where one of the parallel mirrors is allowed to oscillate freely, as shown in Fig.(1). This optomechanical system is driven by two external fields, a control field of frequency ω_c and other a probe field of frequency ω_p, with real amplitudes $\varepsilon_c = \sqrt{2\,\gamma_a\,P_c/\hbar\,\omega_c}$ & $\varepsilon_p = \sqrt{2\,\gamma_a\,P_p/\hbar\,\omega_p}$, respectively, P_c and P_p are the laser powers of the control and probe driving fields, respectively, and γ_a is the cavity decay rate. The coupling in this system is between the cavity field and the mechanical oscillator via the radiation pressure. This optomechanical system total Hamiltonian has the form, [73],

$$\mathcal{H} = \hbar\,\omega_a\,\hat{a}^\dagger\hat{a} + \hbar\,\omega_b\,\hat{b}^\dagger\hat{b}\mathcal{H}_i - \hbar\,\chi\,\hat{a}^\dagger\hat{a}\left(\hat{b}^\dagger + \hat{b}\right) + i\,\hbar\,\varepsilon_c\left(\hat{a}^\dagger\,e^{-i\omega_c t} + \hat{a}\,e^{i\omega_c t}\right) + i\,\hbar\,\varepsilon_p\left(\hat{a}^\dagger\,e^{-i\omega_p t} + \hat{a}\,e^{i\omega_p t}\right) \quad (1)$$

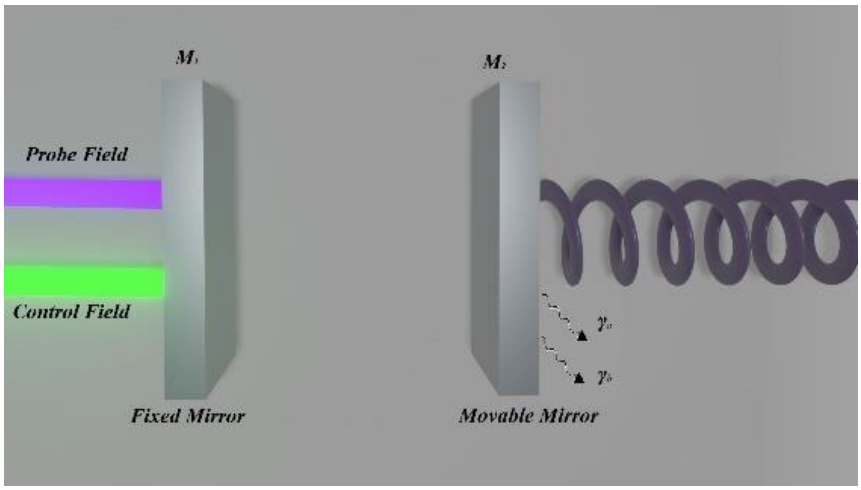

Fig. 1: Schematic diagram for the Simple optomechanical model: M1 and M2 are fixed and movable mirrors, respectively. The strong (control) and probe fields enter the cavity at mirror M1. $\gamma_{a,b}$ are the optical cavity and mechanical decay rates, respectively

where the first term in Eqn.2 represents the cavity field free energy, and $\hat{a}\ (\hat{a}^{\dagger})$ is the annihilation(creation) operator of the cavity field of a frequency ω_a. The second term represents the mechanical mode of vibration-free energy and is expressed in form annihilation(creation) $\hat{b}\ (\hat{b}^{\dagger})$ operator of the mechanical modes of vibration of frequency ω_b. The third term expresses interaction energy resulting from the cavity field mechanical mode coupling due to the radiation pressure. The last two terms are the driving control and probe fields.

In the rotating frame of reference with frequency ω_c(where faster oscillation terms are dropped), the total Hamiltonian, Eqn.1, is given as,

$$\mathcal{H} = \hbar\,\delta_a\,\hat{a}^{\dagger}\hat{a} + \hbar\,\omega_b\,\hat{b}^{\dagger}\hat{b} - \hbar\,\chi\,\hat{a}^{\dagger}\hat{a}\left(\hat{b}^{\dagger} + \hat{b}\right) + i\,\hbar\ \varepsilon_c\,(\hat{a}^{\dagger} - \hat{a}) + i\,\hbar\ \varepsilon_p\left(\hat{a}^{\dagger}\,e^{-i\delta t} - \hat{a}\,e^{i\delta t}\right)$$

Where $\delta_a = \omega_a - \omega_c$ is the detuning frequency ω_a of the cavity field from the frequency ω_c of the driving control field, and $\delta_a = \omega_p - \omega_c$ is the detuning frequency ω_p of the driving probe field from the frequency ω_c of the driving control field.

The Heisenberg-Langevin equations of this simple system are,

$$\frac{\partial a}{\partial t} = -\,\delta_a\,a + i\,\chi\,a\,(\,b^{\dagger} + b) - \varepsilon_c - \varepsilon_p\ e^{-i\delta t} - \gamma_a\,a$$
$$\frac{\partial b}{\partial t} = -\,\omega_b\,b + i\,\chi\,a^{\dagger}a - \gamma_b\,b$$

The nonlinear system of non-autonomous Maxwell-Bloch Eqn.3&4, can be treated via Fourier series decomposition up to the first harmonics in the frequency detuning ($\delta \neq 0$), e.g. see Ref. [40,48]

$$a = \langle\hat{a}\rangle = a_0 + a_+\,e^{i\delta t} + a_-\,e^{-i\delta t}$$
$$b = \langle\hat{b}\rangle = b_0 + b_+\,e^{i\delta t} + b_-\,e^{-i\delta t}$$

In which a_0 and b_0 represent the fundamental component of the cavity field and mechanical modes which is not affected by the probe field ε_p. The first harmonic components $a_{\pm}$ and $b_{\pm}$ are generated in the presence of the detuned weak field $(\varepsilon_p \neq 0)$. We will use the mean value of the parameter in the steady state condition for both the fundamental and first harmonics, of Eqn.3&4, and by using the Fourier decomposition as in Eqn.5&6, and comparing the coefficients up to first harmonics $(e^{-ik\delta t}; for\ k = 0, \pm 1)$ the analytical expressions for the fundamental $(k = 0)$ and in-and out-phase first harmonic components $(k = -, +)$ are givens as following, e.g. see Ref. [74].

(a) Fundamental components (a_0 and b_0)

$$a_0 = \frac{\varepsilon_c}{\left(\gamma_a + i(\delta_a - 2\,\beta_0\,\omega_b\,X_0)\right)}$$

$$b_0 = \frac{\beta_0}{\chi}\,(\omega_b + i\,\gamma_b)\,X_0$$

Where $\beta_0 = \frac{\chi^2}{(\omega_b{}^2 + \gamma_b{}^2)}$ and $X_0 = |a_0|^2$

(b) First harmonic components ($a_\pm$ and $b_\pm$)

$$a_- = \frac{\kappa_1^*\,\varepsilon_p}{(\kappa_1^*\,\kappa_2 - \chi^4\,\alpha_1^2(\delta)\,X_0^2)}$$

$$a_+ = i\,\frac{\chi^2\,\alpha_1^*(\delta)\,a_0{}^2}{\kappa_1}\,a_-^* \qquad \text{I)}$$

$$b_\pm = i\,\frac{\beta_1(\pm\delta)}{\chi}\,(a_0^*\,a_\pm + a_0\,a_\mp^*) \qquad \text{.)}$$

Where $\beta_1(\pm\delta) = \frac{\chi^2}{(\gamma_b + i\,(\omega_b{}^2 \pm \delta))}$,

$\beta_2(\pm\delta) = (\gamma_b{}^2 + (\omega_b \pm \delta)^2\,)$,

$\alpha_1(\delta) = \frac{\omega_b\,(\beta_2(\delta)+\beta_2(-\delta))+(-\delta+i\gamma_b)\,(\beta_2(\delta)-\beta_2(-\delta))}{\beta_2(-\delta)\,\beta_2(\delta)}$,

$\kappa_1 = \gamma_a + i\,(\delta_a + \delta - 2\,\beta_0\,\omega_b\,X_0 - \chi^2\,\alpha_1^*(\delta)\;X_0)$ and $\kappa_2 = \gamma_a + i\,(\delta_a - \delta - 2\,\beta_0\,\omega_b\,X_0 - \chi^2\,\alpha_1(\delta)\;X_0)$.

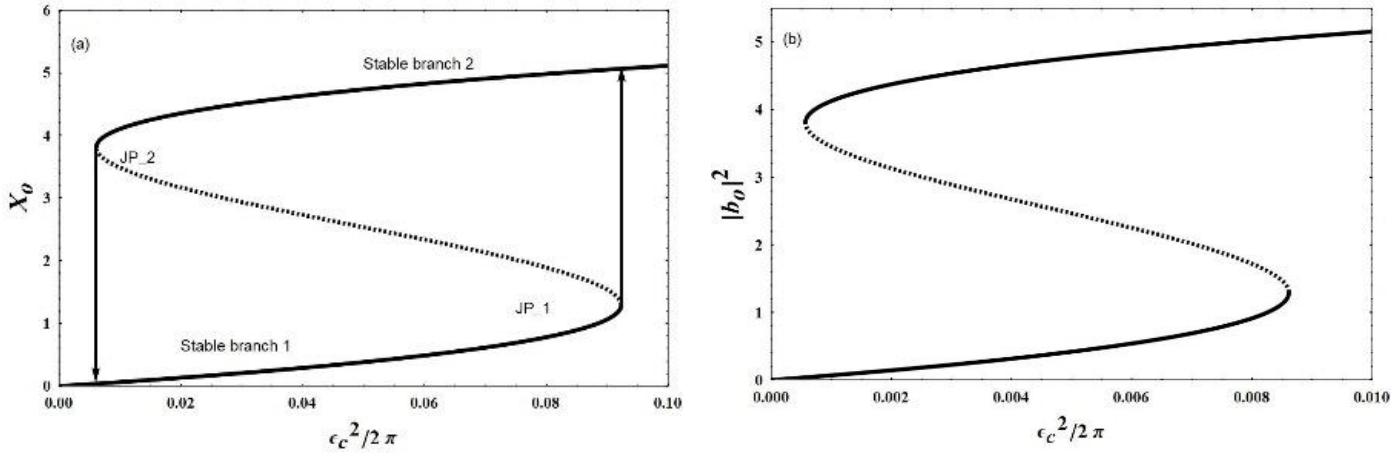

Fig. 2: (a) The average cavity photon number X_0 (in case of $\varepsilon_p = 0$) against the incident field $\frac{\varepsilon_c}{2\,\pi}$ for $\chi = 1.4$, $\delta_a = 1$, $\gamma_a = 0.1$, $\omega_b = 15$ and $\gamma_b = 0.1$. (b) The average mechanical modes $|b_0|^2$ (in case of $\varepsilon_p = 0$) against the incident field $\frac{\varepsilon_c}{2\,\pi}$ for the same parameters as Fig.2(a).

Fig. 2 (a) presents the input-output relation of the cavity output field fundamental component X_0 against the normalized incident field intensity input ${\varepsilon_c}^2/_{2\pi}$, this non-linear relation between the input and the output is an optical bistable relation. In this relation the cavity output field fundamental component X_0 increases linearly with the incident field intensity in the stable branch 1 till it reaches the transition point (JP_1) then it jumps to the upper stable branch 2, if the incident field intensity decreases at this stable branch 2 the cavity output field fundamental component X_0 will follow the curve till it reaches the transition point (JP_2) then at this point the relation makes a jump down to the stable branch 1. The actual bath the system will follow is an anti-clockwise hysteresis loop-shaped relation which is in good agreement with the Experimental results. Fig.2(a,b) shows the similarity of switching behavior in both the input-output relation and the mechanical mode vs. input relation. The bistability appears in the fundamental component of mechanical mode b_0 is dependent on the behavior of the fundamental component of cavity field a_0, as seen from Fig.3(a,b) and also can be deduced from Eqn.8 the linear dependence of b_0 on X_0. Similarly, a dependency will appear for the first harmonic component of both the optical cavity field $a_{\pm}$ and mechanical mode of vibration $b_{\pm}$, as can be deduced from Eqn.(9-11).

As we concluded before all the bistability transition points (i.e. the point at which the system jumps from the lower stable branch to the higher stable or the reverse) have the same incident field intensity position for all components of the optical cavity field and mechanical mode of vibration. All the mechanical modes of vibration components $(b_k; for\ k = 0, \pm 1)$ and the higher harmonics of the optical cavity field $a_{\pm}$ depend on the fundamental optical cavity field component a_0 as we can see in Eqn. (8-11). According to the previous deduction, deriving a mathematical equation that describes the condition needed for each optical bistable behavior to occur for the fundamental component of the optical cavity field and other system variables. Starting from Eqn.7 and by building a functional relation of ε_c^2 function in X_0, we get,

$$\varepsilon_c^2(X_0) = \left({\gamma_a}^2 + {\delta_a}^2\right) X_0 - 4\,\delta_a\,\beta_0\,\omega_b\,{X_0}^2 + 4(\beta_0\,\omega_b)^2\,{X_0}^3 \quad (12)$$

Eqn.12 presents the intensity of the incident field ε_c^2 as a cubic function relation on the fundamental optical cavity field of amplitude X_0. The transition points present in Fig.2 according to Eqn.12 are considered here as the local maximum and local minimum point of the function $\varepsilon_c^2(X_0)$, as seen in Fig.3. Calculating this critical point of the function from finding the roots of this $\left(\frac{d\,\varepsilon_c^2}{dX_0} = 0\right)$ will give us to roots, Which will be as follows,

$$X_0 = \frac{2\,\delta_a \pm \sqrt{4\left({\delta_a}/{\beta_0\,\omega_b}\right) - 3\left({\gamma_a}^2 + {\delta_a}^2\right)}}{3\,(\beta_0\,\omega_b)} \quad (13$$

Calculating the roots in Eqn.13 leads to determining with high precision the optical bistable behavior of our system for certain system parameters. We have three cases for the equation each case describes different behavior; the first case describes the transistor behavior of the optical cavity, which happens $\sqrt{4\left({\delta_a}/{\beta_0\,\omega_b}\right) - 3\left({\gamma_a}^2 + {\delta_a}^2\right)} = 0$ then we get two identical real roots, the next case which is the case of optical bistable behavior as seen in Fig.(2), which happens when $\sqrt{4\left({\delta_a}/{\beta_0\,\omega_b}\right) - 3\left({\gamma_a}^2 + {\delta_a}^2\right)} > 0$ we will get two distinct real roots, finally the monostable case which happens when we get two complex roots where $\sqrt{4\left({\delta_a}/{\beta_0\,\omega_b}\right) - 3\left({\gamma_a}^2 + {\delta_a}^2\right)} < 0$. As seen from the roots in Eqn.13 the relative position of the two roots is controlled by χ coupling constant, ω_b mechanical oscillation, frequency, γ_b the mechanical decay rate, and finally the atomic cavity detuning δ_a, while the distance between the two roots in the case of bistability is controlled by all the cavity parameters.

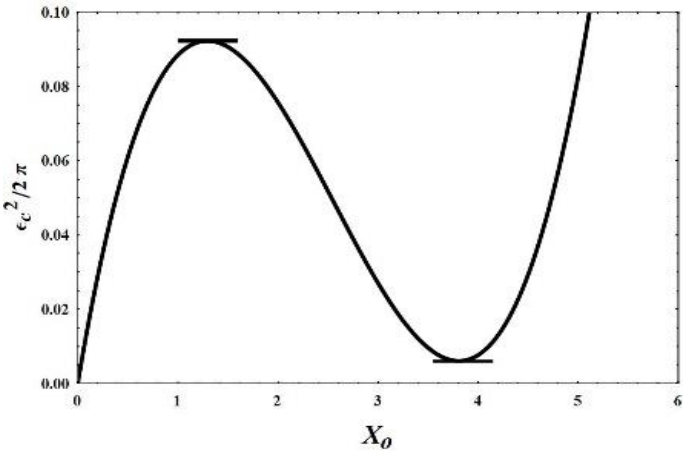

Fig. 3: The incident field $\frac{\varepsilon_c}{2\,\pi}$ (in case of $\varepsilon_p = 0$) against the average cavity photon number X_0 for the same parameters as Fig.2, this graph demonstrates the method of calculating the transition point of the optical bistability in a conventional optomechanical system.

2.2 An ensemble of N 2-level atoms assisted optomechanical system

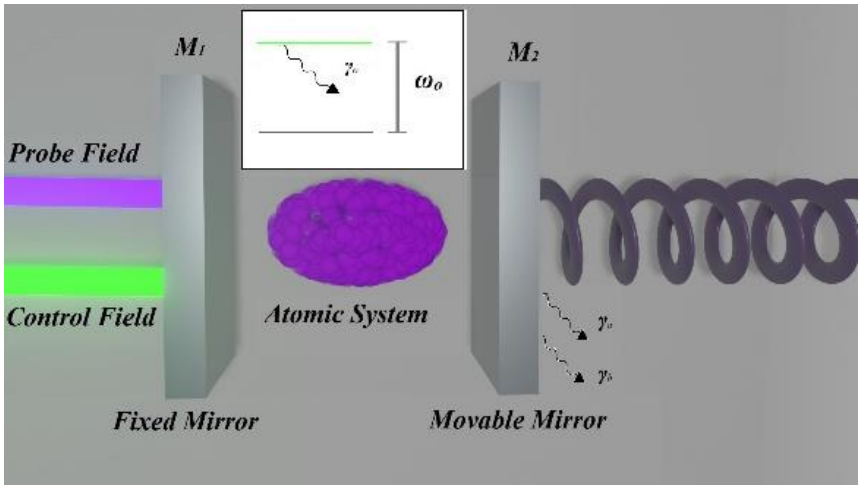

Fig. 4: Schematic diagram for the hybrid optomechanical model: M1 and M2 are fixed and movable mirrors, respectively. The strong (control) and probe fields enter the cavity at mirror M1. $\gamma_{a,b}$ are the optical cavity and mechanical decay rates, respectively. An ensemble of N 2-level atoms with frequency ω_o, coupled to the optical cavity mode.

Here, we will use a hybrid optomechanical model by just entrapping an ensemble of N 2-level atoms trapped in the optical cavity. Similar to ref. [75] the atomic medium is coupled to the cavity field via Jaymes-Cumming coupling. Using a similar system as that referred to in ref. [75], this will lead us to total Hamiltonian in the rotating frame of reference with frequency ω_c, given as,

$$\mathcal{H} = \hbar\,\delta_a\,\hat{a}^\dagger\hat{a} + \hbar\,\omega_b\,\hat{b}^\dagger\hat{b} + {}^{\hbar\,\delta_o}/_2\sum_{i=0}^{N}\hat{\sigma}_z^i - \hbar\,\chi\,\hat{a}^\dagger\hat{a}\,(\hat{b}^\dagger + \hat{b}) + \hbar\,G\sum_{i=0}^{N}(\hat{\sigma}_-^i\,\hat{a}^\dagger + \hat{\sigma}_+^i\,\hat{a}) + i\,\hbar\,\varepsilon_c\,(\hat{a}^\dagger + \hat{a}) + i\,\hbar\,\varepsilon_p\,(\hat{a}^\dagger\,e^{-i\delta t} + \hat{a}\,e^{i\delta t}) \quad (14)$$

Where $\delta_o = \omega_o - \omega_c$ is the detuning frequency ω_o of the atomic medium excitation from the frequency ω_c of the driving control field. To use the Holstein-Primakoff representation [76] our ensemble must be composed of a large number of atoms, this representation will transform the collective atomic operator into annihilation and creation operators $(\hat{A}\ \&\ \hat{A}^\dagger)$, respectively. These operators have the form, $\hat{A} = \frac{1}{N}\sum_{i=0}^{N}\hat{\sigma}_-^i$ & $\hat{A}^\dagger = \frac{1}{N}\sum_{i=0}^{N}\hat{\sigma}_+^i$, and satisfy the standard Bosonic commutation relations, $[\hat{A}, \hat{A}^\dagger] \approx 1, \sum_{i=0}^{N}\hat{\sigma}_z^i = 2\,\hat{A}^\dagger\hat{A} - N$.

The Heisenberg-Langevin equations of this hybrid system are,

$$\frac{\partial a}{\partial t} = -\,\delta_a\,a + i\,\chi\,a\,(b^\dagger + b) - \varepsilon_c - \varepsilon_p\,e^{-i\delta t} - i\,g\,\mathrm{A} - \gamma_a\,a \quad (15)$$

$$\frac{\partial b}{\partial t} = -\,\omega_b\,b + i\,\chi\,a^\dagger a - \gamma_b\,b \quad (16)$$

$$\frac{\partial A}{\partial t} = -\,\delta_o\,b - i\,g\,a - \frac{\gamma_o}{2}\,A \quad (17)$$

where $g = G\sqrt{N}$.

In the previous sub-section, we concluded that all the mechanical modes of the vibration component and the optical cavity field first harmonic component bistability transition points are dependent on the fundamental optical cavity field component. Similarly, all the components of the mechanical mode of vibration, the atomic medium, and the first harmonic of the optical cavity field will be dependent on the fundamental cavity field, see component equation in ref. [75].As we focus on the fundamental cavity field component as it is our main part in studying the system bistability behavior, we will write down the fundamental component of the optical cavity field equation for our hybrid system as follows,

$$a_0 = \frac{\varepsilon_c}{[(\gamma_a + g^2\varphi) + i(\delta_a - g^2\,\eta - 2\,\beta_0\,\omega_b\,X_0)]} \quad (18)$$

where $\varphi = \frac{\delta_o}{\left(\left(\frac{\gamma_o}{2}\right)^2 + {\delta_o}^2\right)}$ and $\eta = \frac{\frac{\gamma_o}{2}}{\left(\left(\frac{\gamma_o}{2}\right)^2 + {\delta_o}^2\right)}$, rewriting Eqn.18 in the functional form as we did in the previous sub-section $\varepsilon_c^2(X_0)$, to calculate the critical point in this case that gives us two roots which will help us to determine the optical behavior of the system, as follow

$$((\gamma_a + g^2\varphi)^2 + (\delta_a - g^2\,\eta)^2)\,X_0 - 4\,(\delta_a - g^2\,\eta)\,\beta_0\,\omega_b\,{X_0}^2 + 4(\,\beta_0\,\omega_b)^2\,{X_0}^3 = \varepsilon_c^2 \quad (19)$$

$$X_0 = \frac{2(\delta_a - g^2\,\eta) \pm \sqrt{(\delta_a - g^2\,\eta)^2 - 3\,(\gamma_a + g^2\varphi)^2}}{6\,(\,\beta_0\,\omega_b)} \quad (20)$$

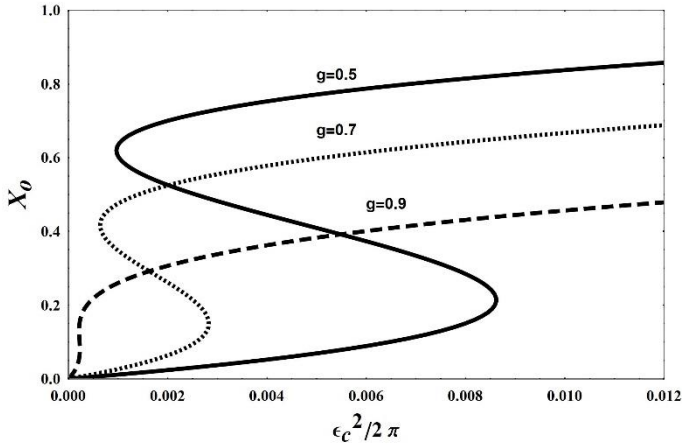

Fig. 5: The average cavity photon number X_0 (in case of $\varepsilon_p = 0$) against the incident field $\frac{\varepsilon_c}{2\,\pi}$ for $\chi = 3$, $\delta_a = 1$, $\gamma_a = 0.1$, $\delta_o = 1, \gamma_o = 0.01$, $\omega_b = 15$, $\gamma_b = 0.1$ and different value of the cavity field atomic medium coupling constant $g = 0.5, 0.7\ \&\ 0.9$.

Eqn. (20), shows that the atomic medium especially the coupling constant g appears in both the relative position of the roots and the distance of the roots. It is seen that the behavior of the system can tuned by varying the atomic medium optical field coupling constant, which is demonstrated in Fig.5. This result is in itself physically acceptable as the atomic medium plays the role of effective amplifier of the cavity field due to the excitation de-excitation processes it performs within the cavity. Fig.5 confirms the effect of coupling constant g on the optical behavior, as for the relation of the input-output fields the bistability switching range turns from a wider range at $g = 0.5$, to a less wide bistability range at $g = 0.7$, and reaches to transistor behavior at $g = 0.9$.

2.3 An ensemble of N 2-level inhomogeneous broadened atoms assisted optomechanical system

Finally, a further modification to the hybrid optomechanical model is considered by entrapping an inhomogeneous broadening ensemble of N 2-level atoms within the optical cavity, as seen in Fig.6 [75]. Using the same system used in ref. [75]. The total Hamiltonian is given as,

$$\mathcal{H} = \hbar\,\delta_a\,\hat{a}^\dagger\hat{a} + \hbar\,\omega_b\,\hat{b}^\dagger\hat{b} + {}^{\hbar\,\delta_o}/_2\sum_{i=0}^{N}\hat{\sigma}_z^i - \hbar\,\chi\,\hat{a}^\dagger\hat{a}\left(\hat{b}^\dagger + \hat{b}\right) + \hbar\,G\sum_{i=0}^{N}(\hat{\sigma}_-^i\,\hat{a}^\dagger + \hat{\sigma}_+^i\,\hat{a}) + i\,\hbar\,\varepsilon_c\,(\hat{a}^\dagger + \hat{a}) + i\,\hbar\,\varepsilon_p\left(\hat{a}^\dagger\,e^{-i\delta t} + \hat{a}\,e^{i\delta t}\right) \quad (21)$$

The cavity field equation is given as

$$a_0 = \frac{\varepsilon_c}{[(\gamma_a + g^2\varphi^{/}) + i(\delta_a - g^2\,\eta^{/} - 2\,\beta_0\,\omega_b\,X_0)]} \quad (22)$$

where $\varphi^{/} = \int_{-\infty}^{\infty} d\nu\,\Pi(\nu)\frac{\nu}{\left(\left(\frac{\gamma_o}{2}\right)^2 + \nu^2\right)}$ and $\eta^{/} = \int_{-\infty}^{\infty} d\nu\,\Pi(\nu)\frac{\frac{\gamma_o}{2}}{\left(\left(\frac{\gamma_o}{2}\right)^2 + \nu^2\right)}$, as $\Pi(\nu)$ is the spectral distribution function of the inhomogeneously broadening. These distribution function will be used as either Gaussian $\Pi_G(\nu)$ Lorentzian $\Pi_L(\nu)$ lineshapes [77].

$$\Pi_G(\nu) = \frac{1}{\sqrt{2\,\pi}\,\sigma_G}\, e^{-\frac{(\nu-\delta_o)^2}{2\,{\sigma_G}^2}} \tag{23}$$

$$\Pi_L(\nu) = \frac{\sigma_L}{2\,\pi}\frac{1}{(\nu-\delta_o)^2+{\sigma_L}^2} \tag{24}$$

As for $\boldsymbol{\sigma_G}$ and $\boldsymbol{\sigma_L}$are the Gaussian and Lorentzian line width parameters, respectively.

Calculating the transition points as in sub-sections (2.1 & 2.2)

$$X_0 = \frac{2\left(\delta_a - g^2\,\eta^{/}\right) \pm \sqrt{(\delta_a - g^2\,\eta^{/})^2 - 3\;(\gamma_a + g^2\varphi^{/})^2}}{6\;(\beta_0\,\omega_b)} \tag{25}$$

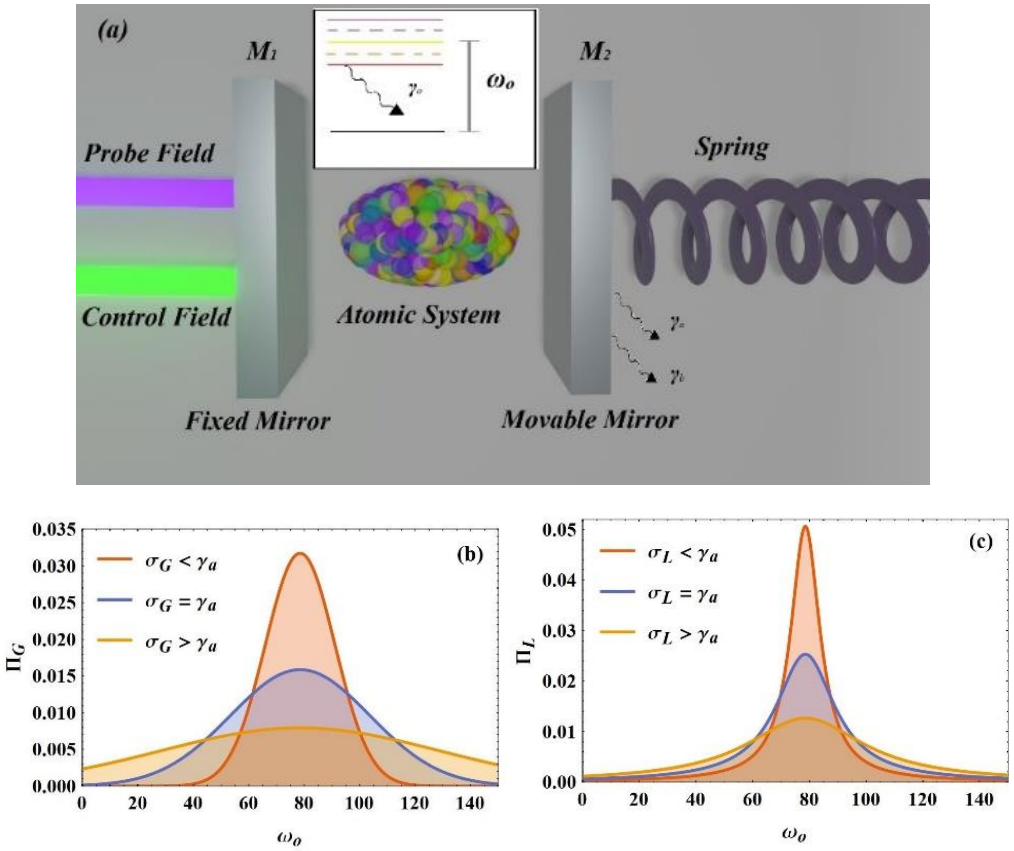

Fig. 6: Schematic diagram for the hybrid optomechanical model: M1 and M2 are fixed and movable mirrors, respectively. The strong (control) and probe fields enter the cavity at mirror M1. $\gamma_{a,b}$ are the optical cavity and mechanical decay rates, respectively. Ensemble of N 2-level inhomogeneously broadened atoms with central frequency ω_o, coupled to the optical cavity mode. (b) & (c) The inhomogeneous lineshape is taken as Gaussian and Lorentzian lineshapes of arbitrary width σ_G and σ_L , respectively, to the cavity decay rate γ_a.

As seen in Fig.7 (a,b) despite using the same parameters that give transistor behavior in the previous sub-section, the inhomogeneous broadening has altered transistor behavior and changed it into bistable behavior by increasing inhomogeneous distribution line widths. The alteration in the behavior happens due to the de-amplification that the inhomogeneous atomic medium performed within the system as a result of its broadened spectral line, so it absorbs cavity photon with detuning δ_a then it remits the photon with different detuning $\delta_a{}^{/}$, this detuning $\delta_a{}^{/}$ have different internal decay rate from the initial detuning δ_a which alter the radiation pressure rate and hence the total behavior of the system.

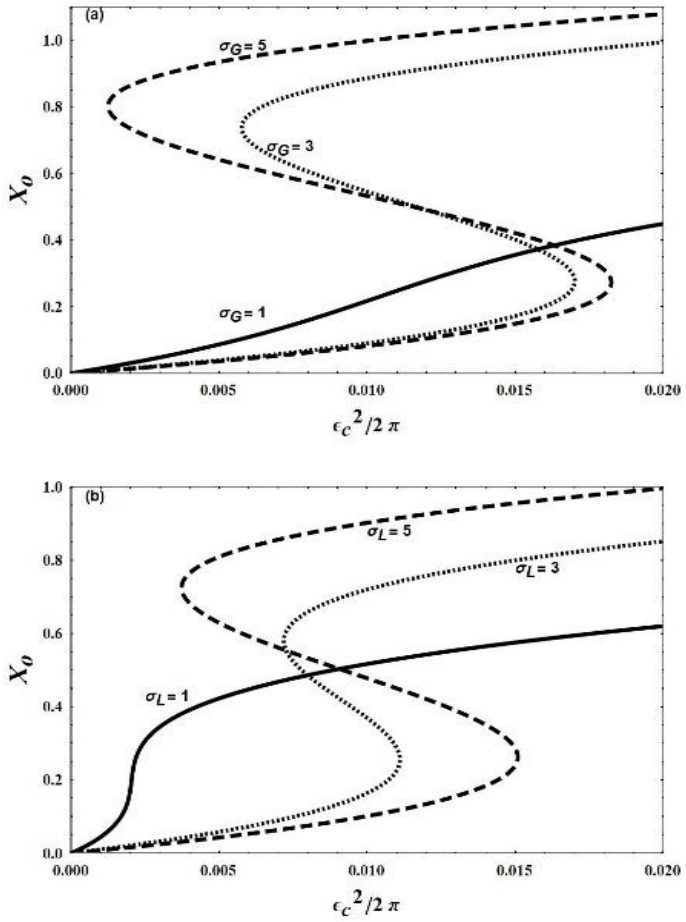

Fig. 7 (a) The average cavity photon number X_0 (in case of $\varepsilon_p = 0$) against the incident field $\frac{\varepsilon_c}{2\pi}$ for $\chi = 3$, $\delta_a = 1$, $\gamma_a = 0.1$, $\delta_o = 1, \gamma_o = 0.01$, $\omega_b = 15$, $\gamma_b = 0.1$ and $g = 0.9$., and different value of Gaussian broadening parameter $\sigma_G = 1, 3 \& 5$. (b) The average cavity photon number X_0 (in case of $\varepsilon_p = 0$) against the incident field $\frac{\varepsilon_c}{2\pi}$ for parameters as Fig.7(a) but for different value of Lorentzian broadening parameter $\sigma_L = 1, 3 \& 5$.

3. Discussion and Conclusion

We began our investigation with a simple optomechanical system, where only the cavity field and the atomic medium interact via radiation pressure. We found that the system parameters can affect the state of the behavior of the system as seen from Eqn. (13). As the system evolves by adding N 2-level atoms trapped within the optical cavity, the system gets more tunable parameters to determine the behavior of the section as presented mathematically in Eqn. (20). The atomic medium plays the role of amplification the effective cavity field from its absorption re-radiation process, this can alter the system and change its behavior from bistable behavior into transistor behavior as presented in Fig.5. Finally by introducing inhomogeneous broadening to the spectral line of the N 2-level atoms, a new tunable parameter the distribution line widths σ was added to control the system behavior. Fig.7 shows the ability of the distribution line widths to reintroduce the bistability behavior into transistor behavior as the case in Fig.5, also Gaussian distribution presents different types of modification of behavior as for Gaussian line width $\sigma_G = 1$ modify the non-broadened system which behaves as transistor into monostable behavior.

Deducing from all we get in the previous section, introducing a 2-level ensemble of atoms modifies the system behavior and adds tunability for optical bistability behavior through the absorption emission process of the atomic medium. A possibility is open for having an optical switching depending on physical parameters such as temperature, as a result of the Doppler broadening shift, which is an inhomogeneous broadening obeying Gaussian distribution shape. Further investigation into controllable atomic medium as quantum dot and double quantum dot will develop more room for switch optoelectrical interface due to the sensitive tuning of the optical bistability by adding atomic medium and the electrical ability to modify the double quantum dot tunneling parameter as ref. [78,79].

References

1. Tittonen, I., G. Breitenbach, T. Kalkbrenner, T. Müller, R. Conradt, S. Schiller, E. Steinsland, N. Blanc, and N. F. de Rooij, 1999, Phys. Rev. A 59, 1038.

2. Gigan, S., H. R. Böhm, M. Paternostro, F. Blaser, G. Langer, J. B. Hertzberg, K. C. Schwab, D. Bäuerle, M. Aspelmeyer, and A. Zeilinger, 2006, Nature Phys. 444, 67.

3. Aspelmeyer, M., Kippenberg, T. J., and Marquardt, F. Springer, (2014).

4. Qvarfort, S., Plato, A. D. K., Bruschi, D. E., Schneiter, F., Braun, D., Serafini, A., and Rätzel, D. Phys. Rev. Research 3, 013159 (2021).

5. Gao, Y.-P., Wang, T.-J., Cao, C., Mi, S.-C., Yang, D., Zhang, Y., and Wang, C. IEEE PhotonicsJournal 9(1), 1–11 (2017).

6. Rogers, B., Gullo, N. L., Chiara, G. D., Palma, G. M., and Paternostro, M. Quantum Measurements and Quantum Metrology 2(1), review 11-43 (2014).

7. Bennett, J. S., Madsen, L. S., Baker, M., Rubinsztein-Dunlop, H., and Bowen, W. P. New Journal of Physics 16(8), 083036 (2014).

8. Bhattacherjee, A. B. and Hasan, M. S. Journal of Modern Optics 65(14), 1688–1697 (2018).

9. Jiang, C., Liu, H., Cui, Y., Li, X., Chen, G., and Shuai, X. Phys. Rev. A 88, 055801 (2013).

10. Ian, H., Gong, Z. R., Liu, Y.-x., Sun, C. P., and Nori, F. Phys. Rev. A 78, 013824 (2008).

11. Xiong, H. and Wu, Y. Applied physics reviews 5(3), 031305 (2018).

12. Xiong, H., Si, L.-G., Zheng, A.-S., Yang, X., and Wu, Y., Phys. Rev. A 86(1), 013815 (2012).

13. Liu, Z.-X., Xiong, H., and Wu, Y. Phys. Rev. A 97, 013801 (2018).

14. Gu, K.-H., Yan, D., Wang, X., Zhang, M.-L., and Yin, J.-Z. Journal of Physics B: Atomic,

Molecular and Optical Physics 52(10), 105502 (2019).

15. Cirio, M., Debnath, K., Lambert, N., and Nori, F. Phys. Rev. Lett. 119, 053601 (2017).

16. Dong Yan , Kai-Hui Gu, Chun-Nian Ren, Li Chen and Jin-Hui Wu, J. Phys. B: At. Mol. Opt.Phys. 51 155003 (2018).

17. Ian, H., Gong, Z. R., Liu, Y.-x., Sun, C. P., and Nori, F. Phys. Rev. A 78, 013824 (2008).

18. Ramos, T., Sudhir, V., Stannigel, K., Zoller, P., and Kippenberg, T. J. Phys. Rev. Lett. 110, 193602 (2013).

19. Bhattacherjee, A. B. and Hasan, M. S. Journal of Modern Optics 65(14), 1688–1697 (2018).

20. Vijay Bhatt et al J. Phys. B: At. Mol. Opt. Phys. 53 155402 (2020).

21. Wang F, Liu W, Wei Z, Meng H, Liu H. Nanomaterials, 11(6):1554 (2021).

22. Ghaffar, A. A., Khan, M. A., Niaz, S., Khan, F., Jamil, M. A., & Ramay, S. M. Int. J. of Quantum Chemistry, 122(17), e26955 (2022).

23. Li, XX., Li, JY., Cheng, XX. et al. Int J Theor Phys 61, 163 (2022).

24. Hamidreza Foroughi and Nader Daneshfara Eur. Phys. J. D 77:118 (2023).

25. Kumar, R., Singh, M.K., Mahajan, S. et al. Opt Quant Electron 56, 91 (2024).

26. Guo, Yujie and Li, Kai and Nie, Wenjie and Li, Yong. Phys. Rev. A 90 5 053841 (2014).

27. Kepler, J., 1619, De Cometis.

28. Einstein, A., 1909, Phys. Z. 10, 817.

29. Cuthbertson, B. D., M. E. Tobar, N. Ivanov E, and D. G. Blair, 1996, Rev. Sci. Inst. 67, 2435.

30. Dorsel, A., J. D. McCullen, P. Meystre, E. Vignes, and H. Walther, 1983, Phys. Rev. Lett. 51, 1550.

31. Braginsky, V. B., and F. Y. A. Khalili, 1995, Quantum Measurements (Cambridge University Press).

32. Braginsky, V. B., and A. B. Manukin, 1977, Measurement of weak forces in Physics experiments (Univ. of Chicago Press).

33. Caves, C. M., 1980, Phys. Rev. Lett. 45, 75.

34. Fabre, C., M. Pinard, S. Bourzeix, A. Heidmann, E. Giacobino, and S. Reynaud, 1994, Phys. Rev. A 49, 1337.

35. Mancini, S., and P. Tombesi, 1994, Phys. Rev. A 49, 4055.

36. Jacobs, K., P. Tombesi, M. Collett, and D. Walls, 1994, Phys. Rev. A 49, 1961.

37. Pinard, M., C. Fabre, and A. Heidmann, 1995, Phys. Rev. A 51, 2443.

38. Cohadon, P.-F., A. Heidmann, and M. Pinard, 1999, Phys. Rev. Lett. 83, 3174.

39. Kleckner, D., and D. Bouwmeester, 2006, Nature (London) 444, 75.

40. Poggio, M., C. L. Degen, H. J. Mamin, and D. Rugar, 2007, Phys. Rev. Lett. 99, 17201.

41. Vogel, M., C. Mooser, K. Karrai, and R. J. Warburton, 2003, Appl. Phys. Lett. 83, 1337.

42. Mertz, J., O. Marti, and J. Mlynek, 1993, Appl. Phys. Lett. 62, 2344.

43. Höhberger, C., and K. Karrai, 2004, in Proceedings of the 4th IEEE Conference on Nanotechnology (IEEE, New York).

44. Zalalutdinov, M., a. Zehnder, a. Olkhovets, S. Turner, L. Sekaric, B. Ilic, D. Czaplewski, J. M. Parpia, and H. G. Craighead, 2001, Appl. Phys. Lett. 79, 695.

45. Höhberger Metzger, C., and K. Karrai, 2004, Nature 432, 1002.

46. Carmon, T., H. Rokhsari, L. Yang, T. J. Kippenberg, and K. J. Vahala, 2005, Phys. Rev. Lett. 94, 223902.

47. Rokhsari, H., T. J. Kippenberg, T. Carmon, and K. J. Vahala, 2005, Opt. Express 13, 5293.

48. Thompson, J. D., B. M. Zwickl, A. M. Jayich, F. Marquardt, S. M. Girvin, and J. G. E. Harris, 2008, Nature (London) 452, 72.

49. Favero, I., S. Stapfner, D. Hunger, P. Paulitschke, J. Reichel, H. Lorenz, E. M. Weig, and K. Karrai, 2009, Opt. Express 17, 12813.

50. Eichenfield, M., R. Camacho, J. Chan, K. J. Vahala, and O. Painter, 2009a, Nature (London) 459, 550.

51. Jiang, X., Q. Lin, J. Rosenberg, K. Vahala, and O. Painter, 2009, Opt. Express 17, 20911.

52. Wiederhecker, G. S., A. Brenn, H. L. Fragnito, and P. S. Russell, 2008, Phys. Rev. Lett. 100, 203903.

53. Ma, R., A. Schliesser, P. Del'Haye, A. Dabirian, G. Anetsberger, and T. Kippenberg, 2007, Opt. Lett. 32, 2200.

54. Park, Y.-S., and H. Wang, 2009, Nature Phys. 5, 489.

55. Tomes, M., and T. Carmon, 2009, Phys. Rev. Lett. 102, 113601.

56. Anetsberger, G., O. Arcizet, Q. P. Unterreithmeier, R. Rivière, A. Schliesser, E. M. Weig, J. P. Kotthaus, and T. J. Kippenberg, 2009, Nature Phys. 5, 909.

57. Brennecke, F., S. Ritter, T. Donner, and T. Esslinger, 2008, Science 322, 235.

58. Murch, K. W., K. L. Moore, S. Gupta, and D. M. Stamper-Kurn, 2008, Nature Phys. 4, 561.

59. A. Szoke, V. Daneu, J. Goldhar, N.A. Kurnit: Appl. Phys. Lett. 15, 376 (1969).

60. J.W. Austin, L.G. Deshazer: J. Opt. Soc. Am. 61, 650 (1971).

61. E. Spiller: J. Appl. Phys. 43,1673 (1972).

62. H. Seidel: US Patent 3,610,731 (1971).

63. S.L. McCall: Phys. Rev. A9, 1515 (1974).

64. H.M. Gibbs, S.L. f~cCall, T.N.C. Venkatesan: Phys. Rev. Lett. 36, 113 (1976).

65. T.N.C. Venkatesan, S.L. McCall: Appl. Phys. Lett. 30, 282 (1977).

66. F.S. Felber, J.H. Marburger: Appl. Phys. Lett. 28, 731 (1976); Phys. Rev. A17, 335 (1978).

67. R. Bonifacio, L.A. Lugiato: Opt. Commun. 19, 172 (1976).

68. R. Bonifacio, L.A. Lugiato: In Coherence and Quantum Optics IV, Proc. 4th Conf. Rochester, USA, June 8-10, 1977, ed. by L. Mandel, F. Wolf (Plenum, New York 1978).

69. R. Bonifacio, L.A. Lugiato: Phys. Rev. AlB, 1129 (1978)

70. Vilson R. Almeida and Michal Lipson. Optics Letters 29, 20, (2004).

71. Andrey A. Nikitin, Ilya A. Ryabcev, Aleksei A. Nikitin, Alexandr V. Kondrashov, Alexander A. Semenov, Dmitry A. Konkin, Andrey A. Kokolov, Feodor I. Sheyerman, Leonid I. Babak, Alexey B. Ustinov. Opt. Com., 511(2022).

72. Yuxiang Peng, Jiao Xu, Hu Dong, Xiaoyu Dai, Jie Jiang, Shengyou Qian, and Leyong Jiang, Opt. Express 28, 34948-34959 (2020).

73. Hui Wang, Xiu Gu, Yu-xi Liu, Adam Miranowicz, Franco Nori, Phys. Rev. A. 90 (2014) 023817.

74. Allen, L. and Eberly, J. H. Optical resonance and two-level atoms, volume 28. Courier Corporation, (1987).

75. Y. A. Sharaby , A. A. Mohamed, I. M. Kandil1 , S. S. Hassan. Optical and Quantum Electronics (2024) 56:1300.

76. Singh, S., Jing, H., Wright, E.M., Meystre, P. Phys. Rev. A 86, 021801 (2012)

77. Y. A. Sharaby, S. Lynch, and S. S. Hassan. J. of Nonlinear Opt. Phys. & Mat. Vol. 2(25) 1650021 (2016).

78. J. M. Villas-Boas, A. O. Govorov, S. E. Ulloa, Phys. Rev. B, 69, 12534 (2004).

79. Y.Amoun, I.Kandil, & A.Ahmed. J Russ Laser Res 42, 512–522 (2021).